Full Text View

Volume 32, Issue 12 (December 2002)

Journal of Physical Oceanography
Article: pp. 3562–3577 | Abstract | PDF (1.85M)

Tracers and Potential Vorticities in Ocean Dynamics

Michael V. Kurgansky*

Department of Atmospheric and Oceanic Physics, Faculty of Physics and Mathematics, University of Concepción, Concepción, Chile

Giorgio Budillon

Institute of Meteorology and Oceanography, University of Naples "Parthenope," Naples, Italy

Ettore Salusti

INFN, Physics Department, University of Rome "La Sapienza," Rome, Italy

(Manuscript received October 6, 2000, in final form June 14, 2002)

DOI: 10.1175/1520-0485(2002)032<3562:TAPVIO>2.0.CO;2

ABSTRACT

The Ertel potential vorticity theorem for stratified viscous fluids in a rotating system is analyzed herein. A set of "tracers," that is, materially conserved scalar quantities, and the corresponding Ertel potential vorticities are used to obtain an absolute fluid velocity determination (including both horizontal and vertical components) that generalizes earlier formulations known in the literature within the framework of the beta-spiral method. Potential vorticity fields, respectively, of (i) density, (ii) potential temperature, (iii) salinity, and (iv) the latter's potential vorticities ratio are analyzed in order to infer properties of steady, or quasi-steady, nonhorizontal or slightly viscous currents. For horizontal flows, general conservative properties of a large class of tracer potential vorticities are found and discussed. These ideas are then applied to various steady cases of physical interest, such as density fronts and thermohaline currents. These arguments, together with observational data, are used to obtain some interesting results, even if the values obtained are affected by large experimental errors. Using this method allows the ratio of the vertical and horizontal components of the velocity field to be estimated with greater certainty. Further insight is also gained into a purely hydrological identification of the no-motion level, a classical difficulty in hydrology.

1. Introduction

Ertel's potential vorticity (EPV in the following) for inviscid fluids is fundamental in geophysical fluid dynamics (Ertel 1942; Gill 1982; Pedlosky 1987; Haynes and McIntyre 1987, 1990; Müller 1995; Salmon 1998; Kurgansky and Pisnichenko 2000). As nicely shown in Müller's (1995) review, principal vorticity and circulation theorems can be inferred from Ertel's theorem. Moreover, EPV

conservation can simplify fluid dynamics analyses. Finally, realistic aspects of physical oceanography are often investigated in terms of EPV (Pedlosky 1987; Rhines 1986; Ripa 1981; Salmon 1982; Cushman-Roisin 1994; and many others as well).

On general grounds, Haynes and McIntyre (1987, 1990) investigated the effect of a realistic friction on EPV evolution. Also Salusti and Serravall (1999) obtained a relation that expresses the evolution of EPV in the presence of mild viscosity and identified novel EPV-related invariants. This relation may be useful both for approximating some particular problems and for diagnosing real current observations. Here we show how similar ideas can be extensively generalized through the application of EPV to oceanic tracer dynamics in order to obtain an absolute velocity determination, and how also rather unexpected properties are obtained for strictly horizontal flows.

In the first instance, the original EPV theorem can be applied to a large family of potential vorticities Π_λ referring to any regular scalar quantity λ. In oceanography a popular choice is to assume that marine water density ρ is materially conserved, namely $D\rho/Dt = 0$ as for incompressible fluids, and thus to assume $\lambda = \rho$ (Müller 1995). In so doing one arrives at the material conservation of the density potential vorticity Π_ρ, valid for incompressible inviscid fluids. So, if both ρ and Π_ρ are conserved, it is the intersection of isopycnals ρ = const with surfaces Π_ρ = const that identifies streamlines. Indeed, the direction of the velocity is known even if its magnitude remains undetermined. However, besides the density ρ, a number of materially conserved quantities such as salinity S, potential temperature θ (for adiabatic flows) and many chemically inert tracers may be found in the oceans. Unlike direct velocity field observations, some of these quantities are relatively easy to measure and interpret (Wunsch 1978).

This naturally raises the general question of whether the "perfect" knowledge of any of these fields, say χ, gives us any additional information of use in determining the fluid velocity. In steady cases, if density and its potential vorticity are materially conserved, the answer is negative since a streamline is identified as the intersection between these two surfaces ρ = const and Π_ρ = const (Fig. 1). There is thus no point in adding that χ = const as it only gives a third plane passing through the streamline, a kind of mathematically degenerate problem.

However, it will be shown that, by considering a tracer χ and its potential vorticity Π_χ with a well-known time evolution, a step toward absolute velocity determination can be made since the Π_χ alongstream evolution in some cases will allow the absolute fluid velocity horizontal and vertical components to be estimated.

This approach and its validity are fully discussed in section 3, taking into account also its relationship with the Needler (1985) equation and with the absolute velocity vector determination outlined by Olbers et al. (1985) according to their beta-spiral method (section 4). It must be borne in mind that the essence of the beta-spiral method involves using two independent tracer conservation equations in order, at any point, to know the direction of the absolute velocity of a current, which has to be essentially baroclinic. The original scheme of Stommel and Schott (1977) uses the thermal wind relation, tracer conservation equations, and also a linearized vorticity balance equation linking vortex stretching and the horizontal advection of planetary vorticity due to the beta term. Olbers et al. (1985) use potential vorticity balance instead of the vorticity equation. All this gives a complex integral–differential relation for the absolute velocity determination, which contains second-order spatial derivatives of the measured tracers. An interesting attempt has been also made by Needler (1985), who obtained from the Bernoulli theorem (cf. Pedlosky 1987; Wunsch 1996) a closed expression for the absolute velocity that is consistent with the beta-spiral method formulation. His tracers are potential density ρ and potential vorticity Π_ρ, and Needler's equation necessarily contains third-order derivatives of the potential density.

In sections 4–6 we investigate properties of tracer potential vorticities respectively related to Π_ρ, that is, Π_{Π_ρ}; potential temperature θ and salinity S, that is, Π_θ, Π_S; and finally of the latter's ratio Π_θ/Π_S. In each case a formula is given for absolute velocity determination, valid for steady inclined baroclinic marine currents. In addition, we show how some combinations of these potential vorticities and of the fluid parcel depth are conserved following horizontal motion, something not previously discussed in the literature. A comparison with velocity measurements in the Ross Sea (Antarctica) is discussed in section 7.

2. Tracers and tracer potential vorticities

Calling $\boldsymbol{\omega}_a$ the absolute vorticity, namely the sum of planetary and relative vorticities (Pedlosky 1987), one has $\boldsymbol{\omega}_a \equiv 2\boldsymbol{\Omega} + \nabla \times \mathbf{u} \equiv 2\boldsymbol{\Omega} + \boldsymbol{\omega}$, where $\mathbf{x}$ is the space position, t the time, $\mathbf{u}$ is the fluid relative velocity and $2\boldsymbol{\Omega} \equiv (0, 0, f)$ is the Coriolis vector. For any scalar quantity $\lambda(\mathbf{x}, t)$ the Ertel theorem gives (Pedlosky 1987)

$$\equiv \quad \varepsilon_1 \quad + \quad \varepsilon_2 \quad + \quad \varepsilon_3, \quad (1)$$

where **F** represents frictional effects.

Since $\rho \equiv \rho(p, \theta, S)$, one has

$$\nabla\lambda \cdot \nabla\rho \times \nabla p = \nabla\lambda \cdot \left(\frac{\partial\rho}{\partial\theta}\nabla\theta + \frac{\partial\rho}{\partial S}\nabla S\right) \times \nabla p, \quad (2)$$

which will play a fundamental role in the following. In addition, for large-scale regular flows $f \gg |\boldsymbol{\omega}|$ and consequently $\boldsymbol{\omega}_a \rightarrow f\mathbf{k}$, with **k** being the unit vertical vector.

In the hydrostatic approximation (1) can be approximated as

$$\varepsilon_2 = \rho^{-3}\nabla\lambda \cdot \nabla\rho \times \nabla p \cong -g\rho^{-2}\nabla\lambda \cdot \nabla\rho \times \mathbf{k}$$

$$\equiv -g\rho^{-2}\mathbf{k} \cdot \nabla\lambda \times \nabla\rho \approx -f\rho^{-2}\nabla\lambda \cdot \frac{\partial}{\partial z}(\rho\mathbf{u}_g),$$

where $\mathbf{u}_g$ is the horizontal velocity in geostrophic approximation.

In general, it is usually assumed that Π_λ is conserved if, and only if, $\varepsilon_1 = 0$, $\varepsilon_2 = 0$, $\varepsilon_3 = 0$, an obviously unnecessarily rigid requirement. Indeed, also a milder relation such as

$$\frac{D}{Dt}\Pi_\lambda = \varepsilon_1 + \varepsilon_2 + \varepsilon_3 = A(t)\Pi_\lambda + G(t)$$

can give a new conserved quantity P_λ that generalizes Π_λ (Salusti and Serraval 1999).

Given the general validity of Eq. (1), it is of some interest to investigate the effect of this Ertel theorem on our understanding of tracer dynamics. Let us first consider one of the many tracers that can be found in the oceans, such as salt, inert chemicals, etc., say $\chi(\mathbf{x}, t)$. If this quantity is neither "created" nor "destroyed" by any biochemical reaction in the marine layers, then the χ-conservation equation gives

$$\frac{D}{Dt}\chi = \frac{\partial}{\partial t}\chi + \mathbf{u} \cdot \nabla\chi = 0. \quad (3)$$

In three-dimensional nonstationary fluid flows a "perfect" knowledge of any three tracers χ_i, $i = 1, 2, 3$, obeying (3) can completely determine the velocity $\mathbf{u} = (u, v, w)$ if, and only if, all gradients $\nabla\chi_i$ are noncomplanar. If a current is stationary, as often happens in oceans, all gradients $\nabla\chi_i$ become complanar, as follows directly from stationary tracer equations

$$\mathbf{u} \cdot \nabla\chi_1 = 0, \qquad \mathbf{u} \cdot \nabla\chi_2 = 0, \qquad \mathbf{u} \cdot \nabla\chi_3 = 0 \quad (4)$$

and can also be seen in Fig. 1 showing the planes α, β, Ψ = const and their intersection, namely a streamline. Every streamline can thus also be considered as the intersection of all the planes χ_i = const, giving the direction of velocity vector **u** but not its magnitude.

However, this opens up the interesting possibility of using essentially nonconservative quantities, but with a well-defined alongstream dynamical evolution, which would help us to determine the velocity field. Thus, the goal of the following sections is to show how these nonconservative quantities can be "tracer potential vorticities" Π_χ, the temporal evolution of which is fixed by the EPV theorem (1), possibly in the presence of frictional effects.

3. Fluid tubes and basic equations

In order to gain some general insight into these problems, let us go back to Vilhelm Bjerknes' classical idea (Godske et al. 1957) that surfaces $\alpha(\mathbf{x}, t)$ = const and $\beta(\mathbf{x}, t)$ = const of two conserved tracers α and β divide the fluid into fluid tubes (Fig. 2), or simply tubes, along which the fluid parcels flow. By definition (α, β) tubes cannot terminate or originate inside the fluid. They can either be closed or end at the fluid boundaries.

In a steady case the mass continuity equation and tracer equations are

$$\nabla \cdot (\rho \mathbf{u}) = 0, \qquad \mathbf{u} \cdot \nabla \alpha = 0, \qquad \mathbf{u} \cdot \nabla \beta = 0. \quad (5)$$

One can moreover show (Wunsch 1996) that (5) implies

$$\rho \mathbf{u} = \Phi(\alpha, \beta)\, \nabla \alpha \times \nabla \beta, \quad (6)$$

where Φ is an arbitrary single-valued function: indeed the vector $\mathbf{u}$ is normal to both $\nabla\alpha$ and $\nabla\beta$, whilst $\rho\mathbf{u}$ is divergence free (Ertel and Kuehler 1949); Φ depends on spatial coordinates $\mathbf{x}$ only implicitly, via α and β. Finally it should be noted that these relations (5)–(6) do not depend on the momentum equations, but only on continuity.

Equation (6) enables both the horizontal and vertical components of the absolute velocity $\mathbf{u}$ to be determined, but a precise measurement of the velocity should be made at least in one point for each streamline, in order to specify the function $\Phi(\alpha, \beta)$. This is not always the best option, so here we discuss another choice that may prove useful when a supplementary third scalar field is known: let us assume that we have some information about a nonconservative quantity $\gamma(\mathbf{x}, t)$, such that $D\gamma/Dt = \Gamma(\mathbf{x}, t)$ where $\Gamma \neq 0$. In a steady case, when

$$\mathbf{u} \cdot \nabla \gamma = \Gamma, \quad (7)$$

Eqs. (6) and (7) give that

$$\mathbf{u} = \frac{\Gamma(\mathbf{x})}{(\nabla\alpha \times \nabla\beta) \cdot \nabla\gamma(\mathbf{x})} \nabla\alpha \times \nabla\beta, \qquad (8)$$

allowing one to obtain $\mathbf{u}$ from a knowledge of α, β, γ, and Γ. In Eq. (7) the dynamics may appear, as it is in (1).

These relations produce two immediate consequences of experimental interest. First, from (8) the ratio of horizontal and vertical velocity components is readily obtained, without any of the experimental uncertainties due to the ratio $\Gamma[(\nabla\alpha \times \nabla\beta) \cdot \nabla\gamma]^{-1}$. Only the gradients of α and β, entering $\nabla\alpha \times \nabla\beta$ in the numerator of (8), contribute to these errors. Second, in cases where some materially conserved tracers are known, such as salinity, potential temperature, and some chemicals, one can tentatively identify the no-motion level by searching for cases where $\nabla\alpha \times \nabla\beta = 0$. In general cases, it may be wrong: it is easy to imagine a barotropic flow with $\nabla\alpha \times \nabla\beta \equiv 0$, with α being the potential-temperature salinity and β the salinity. Nevertheless, for inclined baroclinic or slightly viscous flows, see also below, this idea can work and will be applied to known cases of the Mediterranean Sea in a subsequent paper.

Furthermore, if we consider two fixed α and β tracers and different possible choices (γ, Γ), (γ_1, Γ_1), (γ_2, Γ_2), etc., the resulting velocities $\mathbf{u}$ must be the same, as far as (5)–(8) are exactly verified. But, if we sum or multiply these different (γ, Γ) tracers, interesting properties may be found such as

$$\begin{aligned} \mathbf{u} \cdot \nabla(\gamma + \gamma_1) &= \Gamma + \Gamma_1, \\ \mathbf{u} \cdot \nabla(\gamma\gamma_1) &= \gamma\Gamma_1 + \gamma_1\Gamma, \\ \mathbf{u} \cdot \nabla(1/\gamma) &= -\gamma^2\Gamma, \ldots, \quad (\text{if } 1/\gamma \text{ exists}) \end{aligned} \quad (9)$$

that underline a general algebraic structure of (5)–(8), of some interest in applications.

In addition, it is clear that the hypotheses relative to (5)–(8) are not easily satisfied in realistic problems, as discussed in section 7. We therefore now discuss the limits of validity of our equations (5)–(8). The general case is actually

$$\begin{aligned} \partial_t \alpha + \mathbf{u} \cdot \nabla\alpha &= A', \\ \partial_t \beta + \mathbf{u} \cdot \nabla\beta &= B', \\ \partial_t \gamma + \mathbf{u} \cdot \nabla\gamma &= \overline{\Gamma} + \Gamma' \end{aligned} \qquad (10)$$

for general time- and space-dependent quantities A', B', Γ' that act as sources of α, β, and γ. Clearly, real field observations give values of the various tracers that are not actually constant, but in most cases show time-dependent fluctuations due to external forcing such as atmospheric winds or tides, and also due to fronts, internal waves, turbulence, etc. Nevertheless these tracer variations usually have relatively small amplitude compared with the time-average of the various tracer concentrations. On the other hand, the velocity field $\mathbf{u} = \underline{\mathbf{u}} + \mathbf{u}'$ displays considerable fluctuations $\mathbf{u}'$, often much larger than the time-averaged value of the velocity $\underline{\mathbf{u}}$, as nicely discussed by Wunsch (1978). So the main difference between (5)–(8) and (10) is in the strongly time-varying velocity field $\mathbf{u}'$. Note that, in addition, A' and B' can contain small, steady terms to describe mixing and diffusion of α and β.

In conclusion, we seek a solution for the velocity vector in the form

$$\mathbf{u} = U(\mathbf{x}, t)\nabla\alpha + V(\mathbf{x}, t)\nabla\beta + W(\mathbf{x}, t)(\nabla\alpha \times \nabla\beta), \qquad (11)$$

an absolutely general representation provided that $\nabla\gamma \cdot \nabla\alpha \times \nabla\beta \neq 0$. Setting $A^* = A' - \partial_t\alpha$, $B^* = B' - \partial_t\beta$, and $\Gamma^* = \Gamma' - \partial_t\gamma$ now leads to a general solution

$$\mathbf{u} = \frac{\overline{\Gamma}}{\nabla\gamma \cdot \nabla\alpha \times \nabla\beta}(\nabla\alpha \times \nabla\beta) + \mathbf{u}^* + \frac{\Gamma^* - \mathbf{u}^* \cdot \nabla\gamma}{\nabla\gamma \cdot \nabla\alpha \times \nabla\beta}(\nabla\alpha \times \nabla\beta), \qquad (12)$$

where the first right-hand term corresponds to (8). The second right-hand term describes the velocity of flow towards the tube walls, namely

$$\mathbf{u}^* = U\nabla\alpha + V\nabla\beta,$$

with

$$U = \frac{A^*(\nabla\beta)^2 - B^*(\nabla\alpha \cdot \nabla\beta)}{(\nabla\alpha)^2(\nabla\beta)^2 - (\nabla\alpha \cdot \nabla\beta)^2},$$
$$V = \frac{B^*(\nabla\alpha)^2 - A^*(\nabla\alpha \cdot \nabla\beta)}{(\nabla\alpha)^2(\nabla\beta)^2 - (\nabla\alpha \cdot \nabla\beta)^2}. \qquad (13)$$

Note how it follows from (11)–(13) that

$$\mathbf{u}^* \cdot \nabla\alpha = A^*, \qquad \mathbf{u}^* \cdot \nabla\beta = B^*. \qquad (14)$$

Finally the third right-hand term in (12) provides corrections for the alongtube velocity component.

In general, in (12) for small $\partial_t\alpha$ and $\partial_t\beta$ there is a steady, or quasi-steady, flow related to $\overline{\Gamma}$ and possibly to $\mathbf{u}^* \cdot \nabla\gamma$, superimposed on a time-dependent flow related to $\partial_t\alpha$ and $\partial_t\beta$. In addition, from (12) we see how for small $\partial_t\alpha$ and $\partial_t\beta$ the large velocity fluctuations are essentially due to $\Gamma' - \partial_t\gamma$. All this allows the validity of our Eqs. (11)–(14) to be checked: indeed, if $\partial_t\alpha$, A', $\partial_t\beta$, B', and Γ^* are large, our treatment does not hold and different relations have to be used.

Finally an intuitive depth-dependent representation of potential vorticities for steady flows is discussed. From (8) one easily obtains that

$$\frac{D\gamma}{Dt} = \frac{\nabla\gamma \cdot \nabla\alpha \times \nabla\beta}{\mathbf{k} \cdot \nabla\alpha \times \nabla\beta}\frac{Dz}{Dt}. \qquad (15)$$

Particularly interesting general solutions of (15) are

$$\gamma = F(\alpha, \beta)L(z) + G(\alpha, \beta), \qquad (16)$$

valid for arbitrary functions L, F, and G, as long as $\nabla\alpha$, $\nabla\beta$, and $\mathbf{k} = \nabla z$ are not complanar. Equation (16) shows how inside an inclined (α, β) tube, each γ value can be seen as a mere function of z. Consequently a combination of γ and z becomes a constant of motion.

4. Applications to the density field

The most natural example to consider is to take γ as a radioactive isotope concentration with $\mathbf{u} \cdot \nabla\gamma = \Gamma = -\Lambda\gamma$, where $\tau = \Lambda^{-1}$ is the temporal decrement of radioactive decay (Roether et al. 1999; England and Maier-Reimer 2001). This point is intended to form the basis of a forthcoming study.

Let us now analyze incompressible inviscid fluids: following Needler (1985) we set $\alpha = \rho$, $\beta = \Pi_\rho$, and $\gamma = \Pi_\beta$ to extract all the possible information from the density field alone. Thus Eq. (15) implies that the streamlines lie along the intersections

of ρ = const and Π_ρ = const surfaces (Olbers et al. 1985; Marshall et al. 1993).

From the EPV theorem for such incompressible inviscid currents it follows that

$$\frac{D}{Dt}\Pi_\beta \equiv \frac{D}{Dt}\left(\frac{\boldsymbol{\omega}_a \cdot \boldsymbol{\nabla}\Pi_\rho}{\rho}\right) = \frac{\boldsymbol{\nabla}\Pi_\rho \cdot \boldsymbol{\nabla}\rho \times \boldsymbol{\nabla}p}{\rho^3} = \Gamma, \qquad (17)$$

which is generally not zero. In a hydrostatic steady case, all this yields

$$\mathbf{u} = -\frac{g\rho^{-2}\boldsymbol{\nabla}\Pi_\rho \cdot \boldsymbol{\nabla}\rho \times \mathbf{k}}{\boldsymbol{\nabla}\left(\frac{\boldsymbol{\omega}_a \cdot \boldsymbol{\nabla}\Pi_\rho}{\rho}\right) \cdot \boldsymbol{\nabla}\rho \times \boldsymbol{\nabla}\Pi_\rho}(\boldsymbol{\nabla}\rho \times \boldsymbol{\nabla}\Pi_\rho) \cong \frac{g}{\rho^2}\frac{w}{\mathbf{u} \cdot \boldsymbol{\nabla}(\boldsymbol{\omega}_a \cdot \boldsymbol{\nabla}\Pi_\rho/\rho)}(\boldsymbol{\nabla}\rho \times \boldsymbol{\nabla}\Pi_\rho). \qquad (18)$$

(Click the equation graphic to enlarge/reduce size)

Interestingly, Π_β and $\mathbf{u}$ are proportional to the vertical velocity w. Note also that, if $w \to 0$, we have from (18) that $(\mathbf{u} \cdot \boldsymbol{\nabla}\Pi_\beta)\,\mathbf{u} \to 0$. So, either $\mathbf{u} \cdot \boldsymbol{\nabla}\Pi_\beta \to 0$ or $\mathbf{u} \to 0$, but in the last case $w \propto \mathbf{u}^2$, which is not possible since, for $w \to 0$, one has $\mathbf{u}^2 = u^2 + v^2 + w^2 \approx u^2 + v^2 \neq Cw$ (C is a constant). So for $w \to 0$ one has that $\mathbf{u} \cdot \boldsymbol{\nabla}\Pi_\beta \to 0$ and in (18) $\mathbf{u}$ is consequently an undetermined quantity. On physical grounds this means that for horizontal inviscid flows, with $w = 0$, Π_β does not vary along the streamline, as follows directly also from Ertel's theorem. This is probably the fundamental reason for some difficulties being encountered in applying Needler's (1985) relation.

In general, the last member of (18) may appear as highly nonlinear because of the concomitant effect of w, $\mathbf{u}$, $|\mathbf{u}|$, and so on. This difficulty can be solved by approximating $w/|\mathbf{u}|$ from experimental knowledge of the current pathway. For instance, one can identify the slope of the intersection of ρ = const and Π_ρ = const surfaces or, in order to diagnose density currents, the bottom inclination beneath the current.

For large-scale currents, this equation (18) can be simplified to give

$$\Pi_\rho = \frac{1}{\rho}(2\boldsymbol{\Omega} + \boldsymbol{\nabla} \times \mathbf{u}) \cdot \boldsymbol{\nabla}\rho \approx \frac{1}{\rho}2\boldsymbol{\Omega} \cdot \boldsymbol{\nabla}\rho \cong f\frac{\partial}{\partial z}\ln\rho = -\frac{f}{g}N^2, \qquad (19)$$

$$\Pi_\beta = \frac{(2\boldsymbol{\Omega} + \boldsymbol{\nabla} \times \mathbf{u})}{\rho} \cdot \boldsymbol{\nabla}\Pi_\rho \approx \frac{2\boldsymbol{\Omega}}{\rho} \cdot \boldsymbol{\nabla}\Pi_\rho \approx \frac{f}{\rho}\frac{\partial}{\partial z}\Pi_\rho \cong -\frac{f^2}{g\rho}\frac{\partial}{\partial z}N^2 \equiv -\frac{\Pi_{fN^2}}{g}, \qquad (20)$$

and finally

$$\mathbf{u}(\mathbf{x}) \approx \frac{g}{\rho^2}\frac{\mathbf{k} \cdot \boldsymbol{\nabla}\rho \times \boldsymbol{\nabla}(fN^2)}{\boldsymbol{\nabla}\left(\frac{f^2}{\rho}\frac{\partial}{\partial z}N^2\right) \cdot \boldsymbol{\nabla}\rho \times \boldsymbol{\nabla}(fN^2)}[\boldsymbol{\nabla}\rho \times \boldsymbol{\nabla}(fN^2)] \cong \frac{g}{\rho^2}\frac{w}{\mathbf{u} \cdot \boldsymbol{\nabla}\left(\frac{f^2}{\rho}\frac{\partial}{\partial z}N^2\right)}[\boldsymbol{\nabla}\rho \times \boldsymbol{\nabla}(fN^2)], \qquad (21)$$

where N is the Brunt–Väisälä frequency. The last expression is the well-known Needler's (1985) formula, involving third-

order space derivatives of ρ. Using (21), the density can be inverted (Müller 1995).

Equations (15) and (16) applied to this kind of streamtube give

$$\Pi_{fN^2} \equiv \frac{f^2}{\rho}\frac{\partial}{\partial z}N^2 = F(\rho, fN^2)L(z) + G(\rho, fN^2), \quad (22)$$

with L, F, and G as arbitrary functions. So, inside a given inclined fluid tube Π_{fN^2} is a function of z only. For a special choice of L, F, and G some illuminating analytical **u** representations are discussed in appendix A. For steady motions, in hydrostatic approximation we have

$$\frac{D}{Dt}\Pi_{fN^2} \propto w,$$

which leads to Π_{fN^2} constancy for steady horizontal and slightly viscous motions.

Furthermore, (22) allows an interesting simplification of (21), namely

$$\begin{aligned}\mathbf{u} &= \frac{g}{\rho^2}\frac{\boldsymbol{\nabla}\rho \times \boldsymbol{\nabla}(fN^2)[\mathbf{k}\cdot\boldsymbol{\nabla}\rho \times \boldsymbol{\nabla}(fN^2)]}{\dfrac{\partial}{\partial z}\left(\dfrac{f^2}{\rho}\dfrac{\partial N^2}{\partial z}\right)\mathbf{k}\cdot\boldsymbol{\nabla}\rho \times \boldsymbol{\nabla}(fN^2)} \\ &= \frac{g}{\rho^2}\frac{\boldsymbol{\nabla}\rho \times \boldsymbol{\nabla}(fN^2)}{\dfrac{\partial}{\partial z}\left(\dfrac{f^2}{\rho}\dfrac{\partial}{\partial z}N^2\right)} \end{aligned} \quad (23)$$

since, in general,

$$\boldsymbol{\nabla}F(\alpha, \beta, z) = \frac{\partial F}{\partial \alpha}\boldsymbol{\nabla}\alpha + \frac{\partial F}{\partial \beta}\boldsymbol{\nabla}\beta + \frac{\partial F}{\partial z}\mathbf{k}.$$

This formulation is, interestingly, related only to local quantities since both the vector product and the second vertical derivative of N^2 are measurable in a single transect. So in the following we will call this kind of formula “local.”

In short, although we obtained some useful properties of Π_{fN^2} we also had to overcome the basic difficulty that, even if ρ is not a dramatically varying function, then Π_ρ can be affected by a quickly varying velocity field. In addition, the gradients of p, ρ, N^2, and $\partial N^2/\partial z$ are all comparatively similar functions, even if we are sure that their triple vector products do not vanish. So, it is the fine structure of the potential density field that rules the velocity amplitudes, and this could represent a practical difficulty when field measurements do not give clear enough information about these quantities (Wunsch 1978). Consequently, the approximations outlined in (17)–(23) cannot always be used, which represents a basic difficulty affecting this kind of tracers, such as density and its potential vorticity.

5. Importance of T–S tubes

The preceding difficulties concerning potential density raise some fundamental questions. For instance, could we use information about an additional tracer, say χ, to obtain a relation similar to Needler's formula but avoiding third-order space derivatives, often producing large experimental errors? The answer is affirmative: indeed, let us take $\alpha = \rho$, $\beta = \chi$, $\gamma = \Pi_\chi$. In hydrostatic approximation we thus obtain

$$\approx \frac{g}{\rho^2}\frac{}{\mathbf{u}\cdot\nabla\left(\frac{f}{\rho}\frac{\partial\chi}{\partial z}\right)}(\nabla\rho\times\nabla\chi)$$

$$\approx \frac{g}{\rho^2}\frac{\nabla\rho\times\nabla\chi}{\frac{\partial}{\partial z}\left(\frac{f}{\rho}\frac{\partial\chi}{\partial z}\right)}, \tag{25}$$

the latter being the local equation. Note that we again obtain the interesting property that $D\Pi_\chi/Dt \propto w$, thus showing that each Π_χ is constant for purely horizontal or slightly viscous currents, a feature of some general interest.

For steady adiabatic flows from (2) it is natural to assume that χ is the salinity S or the potential temperature θ. This would also enable one to use more complete information about θ and S, as obtained from in situ measurements. So, in general, we now analyze an adiabatic inviscid current with materially conserved potential temperature and salinity, assuming $\alpha = \theta$, $\beta = S$, $\gamma = \Pi_\theta$. In hydrostatic approximation we have

$$\mathbf{u} = -\frac{g\rho^{-2}(\partial\rho/\partial\theta)\nabla S\cdot\nabla\theta\times\mathbf{k}}{\nabla\left(\frac{\boldsymbol{\omega}_a\cdot\nabla S}{\rho}\right)\cdot\nabla\theta\times\nabla S}(\nabla\theta\times\nabla S)$$

$$\equiv \frac{g}{\rho^2}\frac{w(\partial\rho/\partial\theta)}{\mathbf{u}\cdot\nabla\Pi_S}(\nabla\theta\times\nabla S)$$

$$\approx \frac{g}{\rho^2}\frac{\partial\rho/\partial\theta}{\partial\Pi_S/\partial z}\nabla\theta\times\nabla S, \tag{26}$$

the last equation giving a local value. For a viscous fluid one instead has

$$\mathbf{u} = \frac{\rho^{-3}(\partial\rho/\partial\theta)\nabla p\cdot\nabla\theta\times\nabla S}{\nabla\Pi_S\cdot\nabla\theta\times\nabla S}(\nabla\theta\times\nabla S)$$

$$+\frac{\rho^{-1}\nabla S\cdot\nabla\times(\mathbf{F}/\rho)}{\nabla\Pi_S\cdot\nabla\theta\times\nabla S}(\nabla\theta\times\nabla S), \tag{27}$$

written in general form without the hydrostatic approximation. The presence of the viscous correction in (27), as in the other case to be discussed (29), are of fundamental importance since it allows the preceding considerations to be extended to slightly viscous fluids, also for horizontal flows. Indeed for horizontal flows the first right-hand term in (27) is zero and the main term is the viscous correction. This could be essential in order to identify the no-motion level, where the inviscid formulation (26) could give confusing results.

Two different absolute velocity determinations, namely for $\{\theta, S, \Pi_\theta\}$ like (26) and (27) and for $\{\theta, S, \Pi_S\}$ as below:

$$\mathbf{u} = -\frac{g\rho^{-2}(\partial\rho/\partial S)\nabla\theta\cdot\nabla S\times\mathbf{k}}{\nabla\left(\frac{\boldsymbol{\omega}_a\cdot\nabla\theta}{\rho}\right)\cdot\nabla\theta\times\nabla S}(\nabla\theta\times\nabla S)$$

$$\equiv -\frac{g}{\rho^2}\frac{w(\partial\rho/\partial S)}{\mathbf{u}\cdot\nabla\Pi_\theta}(\nabla\theta\times\nabla S)$$

$$\approx -\frac{g}{\rho^2}\frac{\partial\rho/\partial S}{\partial\Pi_\theta/\partial z}\nabla\theta\times\nabla S, \tag{28}$$

the last being a local value, and for a viscous fluid,

$$\mathbf{u} = \frac{\rho^{-3}(\partial\rho/\partial S)\nabla p \cdot \nabla\theta \times \nabla S}{\nabla\Pi_\theta \cdot \nabla\theta \times \nabla S}(\nabla\theta \times \nabla S) + \frac{\rho^{-1}\nabla\theta \cdot \nabla \times (\mathbf{F}/\rho)}{\nabla\Pi_\theta \cdot \nabla\theta \times \nabla S}(\nabla\theta \times \nabla S) \qquad (29)$$

must result at the same vector **u** for every dynamically possible case of θ and S. Indeed, subtracting (29) from (26) for steady currents of incompressible fluids shows that these two formulations are equivalent since, for $c^2 = \partial\rho/\partial p \longrightarrow \infty$ from (26)–(28), we have

$$\mathbf{u} \cdot \left(\frac{\partial\rho}{\partial S}\nabla\Pi_S + \frac{\partial\rho}{\partial\theta}\nabla\Pi_\theta\right) = \mathbf{u} \cdot \left(\nabla\Pi_\rho - \frac{\partial\rho}{\partial p}\nabla\Pi_p\right) = \frac{D}{Dt}\Pi_\rho = 0.$$

We again stress that both θ and S are the tracers that are most often observed in field measurements. So the aforementioned ratio of horizontal and vertical velocity components is best obtained from these (26)–(29) relations, which are valid also in the case that mild friction must be taken into consideration. Again, similar considerations hold also for the search of the hydrologic no-motion level.

To get some idea of the practical applicability of these relations (26)–(29), in appendix B we discuss a classical density current, that of salty dense Mediterranean Water that crosses the deepest part of the Strait of Gibraltar and flows towards the Atlantic Ocean (Baringer and Price 1997a,b). More in detail, this density current flows along the local topography into the Atlantic Ocean (Fig. 3). Between the hydrological sections B and D the current turns northward with a curvature radius of $R \sim 40$ km; beyond these sections the flow is essentially rectilinear. From sections A to F, over an irregular sea bottom, the current thickness h and its width W are found to increase while the velocity **u** and density difference $\Delta\rho$ compared with the surrounding water masses decrease as the current moves off Gibraltar (Table 1). From (26)–(29) the velocity is obviously along the θ = const and S = const surfaces, even if friction is considered. The velocity intensity is ruled by the gradients of θ, S, as well as by **F**. In Table 1 we show how the nonlocal **u** estimates obtained from Eq. (26) fit the experimental data satisfactorily, while the local **u** computations are affected by errors that are difficult to estimate. In addition, the viscous corrections are seen to be smaller than the estimates of experimental errors.

6. The ratio Π_θ/Π_S and its dynamical properties

This general symmetry between θ and S suggests the utility of a further possibility, namely $\alpha = \theta$, $\beta = S$, $\gamma = \Pi_\theta/\Pi_S$, an element of the algebra (9) generated by Π_S and Π_θ. A somewhat analogous construction, the ratio of EPV and the magnetic analogue of EPV, was introduced by Hide (1996) in a magnetohydrodynamics context. We limit the present analysis to inviscid flows; from (1) we obtain

$$\frac{D}{Dt}\left(\frac{\Pi_\theta}{\Pi_S}\right) = \frac{1}{\rho^3}\frac{\frac{\partial\rho}{\partial S}\Pi_S + \frac{\partial\rho}{\partial\theta}\Pi_\theta}{\Pi_S^2}(\nabla p \cdot \nabla\theta \times \nabla S) \cong -\frac{g}{\rho^2}\frac{\frac{\partial\rho}{\partial S}\Pi_S + \frac{\partial\rho}{\partial\theta}\Pi_\theta}{\Pi_S^2}(\mathbf{k} \cdot \nabla\theta \times \nabla S)$$
$$\approx -\frac{g}{\rho^2}\frac{\Pi_\rho - (\partial\rho/\partial p)\Pi_p}{\Pi_S^2}\frac{w}{|\mathbf{u}|} \underset{c\to\infty}{\approx} -\frac{g}{\rho^2}\frac{\Pi_p}{\Pi_S^2}\frac{w}{|\mathbf{u}|}; \qquad c^{-2} = \frac{\partial\rho}{\partial p}. \qquad (30)$$

(Click the equation graphic to enlarge/reduce size)

Therefore we again have $(D/Dt)(\Pi_\theta/\Pi_S) \propto w$, so for purely horizontal flows Π_θ/Π_S is constant. Also of interest is the fact that for inclined flows the ratio Π_θ/Π_S takes on a particularly elegant form:

$$\frac{\Pi_\theta}{\Pi_S} \approx \frac{\frac{f}{\rho}\frac{\partial\theta}{\partial z}}{\frac{f}{\rho}\frac{\partial S}{\partial z}} = \frac{\partial\theta/\partial z}{\partial S/\partial z} \qquad (31)$$

in a quasigeostrophic approximation, so $\Pi_\theta/\Pi_S \approx (\partial\theta/\partial z)/(\partial S/\partial z)$ remains invariant also in the course of extended meridional

excursions of ocean water masses when f changes because of the β effect. So, (31) shows how Π_θ/Π_S changes deterministically because of the sole effect of baroclinicity, as described by the term $\mathfrak{E}_2$ in Eq. (1). In addition, Π_θ/Π_S can easily be computed from a single CTD cast as $\Delta\theta/\Delta S$, using finite differences to approximate vertical derivatives.

For inclined steady motions one ultimately has

$$\mathbf{u} = \frac{1}{\rho^3 \Pi_S^2} \frac{\left(\Pi_\rho - \frac{1}{c^2}\Pi_p\right)\nabla p \cdot \nabla\theta \times \nabla S}{\nabla\left(\frac{\Pi_\theta}{\Pi_S}\right) \cdot \nabla\theta \times \nabla S} (\nabla\theta \times \nabla S). \quad (32)$$

In addition from (15) and (16) one has

$$\frac{\Pi_\theta}{\Pi_S} \approx \frac{\partial\theta/\partial z}{\partial S/\partial z} = F(\theta, S)L(z) + G(\theta, S)$$

with arbitrary functions F, L, and G. So, inside a (θ–S) tube, Π_θ/Π_S is a function only of the depth z, and the local version of (32) is

$$\mathbf{u} \approx \frac{N^2}{f} \frac{\mathbf{k} \cdot \nabla\theta \times \nabla S}{\left(\frac{\partial S}{\partial z}\right)^2 \frac{\partial}{\partial z}\left(\frac{\partial\theta/\partial z}{\partial S/\partial z}\right) \mathbf{k} \cdot \nabla\theta \times \nabla S} (\nabla\theta \times \nabla S)$$

$$= \frac{1}{f} \frac{N^2}{\left(\frac{\partial S}{\partial z}\right)^2 \frac{\partial}{\partial z}\left(\frac{\partial\theta/\partial z}{\partial S/\partial z}\right)} (\nabla\theta \times \nabla S). \quad (33)$$

This can be compared directly to Needler's (1985) classical result (21). Unlike (21), this equation (33) involves only second-order derivatives of θ and S, which is a definite advantage since θ and S are known more exactly and have richer space variability than the other quantities in (21), as illustrated above.

To examine the relation (33) more properly, we define a pseudovector $\mathbf{U} = [U(z), V(z), 0]$ with horizontal components $U = \partial\theta/\partial z$ and $V = \partial S/\partial z$. In (33) the quantity

$$H = \left(\frac{\partial S}{\partial z}\right)^2 \frac{\partial}{\partial z}\left(\frac{\partial\theta/\partial z}{\partial S/\partial z}\right) = \mathbf{k} \cdot \left(\frac{\partial \mathbf{U}}{\partial z}\right) \times \mathbf{U}$$

$$\equiv \mathbf{U} \cdot \nabla \times \mathbf{U}$$

stands for the rate of change of direction of $\mathbf{U}$ with z: indeed, one can likewise write

$$H = -(U^2 + V^2) \arctan\frac{V}{U} = -\mathbf{U}^2 \frac{\partial\phi}{\partial z}, \quad (34)$$

where ϕ is the angle (measured anticlockwise) between $\mathbf{U}$ and a fixed direction in the horizontal plane. If $\mathbf{U}$ were the horizontal velocity vector, then H could be called the kinematic helicity (Hide 1989); in our case we call H the "thermohaline helicity."

In order to estimate water velocity, H has to be computed. Note how (33) fails when $H = 0$; that is, the vector $\mathbf{U}$ changes only in magnitude with depth, but not in direction. In particular, this failure occurs when $\partial\theta$;cl∂z and $\partial S/\partial z$ are substantially nonzero and vary with depth, but their ratio remains constant. So, absolute velocity determinations based on Eq. (33) should be restricted to a range of depths with $H \neq 0$. The marine currents, which satisfy this necessary condition, may very well be considered essentially as thermohaline currents.

In practical calculations of section 7, in order to avoid large experimental errors coming from taking second vertical derivatives of θ and S in (34), we shall approximate H with its space-averaged value, as also hydrological velocity estimates

are related to space averages. Plotting the **U** hodograph and estimating the area swept up by the **U** vector facilitates this procedure.

7. The Ross Sea dataset

It must be stressed that practical applications of the above relations are not an easy task in the open sea. Indeed, in this approach we are forced to assume that

1. the flow is steady, or at least quasi-steady;
2. there are enough detailed observations of two distinct, materially conserved tracers; and
3. one can identify a tracer potential vorticity with a well-known time or space evolution.

These requirements are not easy to satisfy. Indeed, as a realistic concluding example we now analyze current meter and hydrologic data obtained in the Ross Sea (Antarctica) during the CLIMA Project (Budillon et al. 2002) relative to a current flowing over the continental shelf. To study a flow that is clearly not horizontal we use θ–S data for stations 87 and 88 of transect D, and for stations 89 and 90 of transect E (Fig. 4) positioned at 75°S (transect D) and half a degree (~ 55 km) north (transect E). Stations 88 and 90 were located at ~ 19 km and ~ 24 km, respectively, west of stations 87 and 89 (Table 2).

The hydrologic data (Fig. 5) show in all transects A–E the northward flow of a particularly dense cold water mass, the "Deep Ice Shelf Water" (DISW), beneath another cold lighter water, the "Low Salinity Shelf Water" (LSSW). Using mass conservation properties, Budillon et al. estimated the northward DISW velocity as 8 cm s^{-1} at the bottom transect D, with errors that were rather difficult to define, probably 2–3 cm s^{-1}. No similar estimate was however possible in transect E since DISW was no longer clearly identifiable. On the other hand, in the western part of both transects a warmer water was also observable, the Circumpolar Deep Water (CDW). The northward velocity of CDW is smaller than that of the bottom DISW; it is ~ 4 cm s^{-1}, with an overall error of 3–4 cm s^{-1}. So some rather large spatial gradients, both vertical and horizontal, of the northward velocity must have been present.

In addition direct current meter data show that the mean flow in the mooring $\tilde{H}$, south of transect D (shown in Fig. 4), was directed northeastwards at all depths at a velocity of 3–4 cm s^{-1}. In particular the most superficial current meter, at a depth of 282 m, gave a northward horizontal velocity of ~ 6.3 cm s^{-1} during the CTD observation time (July 1995).

From vertical density profiles for stations 87–90 we found an evident velocity variation in transect D at a depth of ~ 50 m, so we focused our attention on deeper layers around a streamtube present in both D and E transects bounded by surfaces $\theta = -1$, −0.4°C and $S = 34.3$, 34.5 psu. Its mean depth is ~ 75 ± 10 m in transect D and ~ 120 ± 10 m in transect E: so moving northward this current deepens by ~ 40 m over 55 km: this gives a ratio of vertical and alongstream velocities $w/v \sim -7 \times 10^{-4}$, with an error of 20%.

For this streamtube, in the more regular transect D we estimated

$$(\nabla\theta \times \nabla S)_x = (4 \pm 1) \times 10^{-9}\,^{\circ}\mathrm{C\ psu\ m^{-2}},$$

$$(\nabla\theta \times \nabla S)_y = (13 \pm 2) \times 10^{-8}\,^{\circ}\mathrm{C\ psu\ m^{-2}},$$

$$(\nabla\theta \times \nabla S)_z = -(5 \pm 1) \times 10^{-11}\,^{\circ}\mathrm{C\ psu\ m^{-2}}, \quad (35)$$

where the x axis is directed westward, the y axis northward, and the z axis upward. The errors in the gradients in (35) were rather difficult to estimate: we assumed that θ and S between two stations is the linear interpolation of the observed values. So the relative errors here are assumed as that of the majority of hydrologic measurements, namely ~ 10%. From these (35) the ratio w/v can be estimated as -4×10^{-4}, with an error of 40%, in agreement with the previous estimate.

To check the applicability of this method, from (33) we computed

$$v = \frac{N^2}{fH}(\nabla\theta \times \nabla S)_y \quad (36)$$

with $H \neq 0$ given by (34). The northward component $(\nabla\theta \times \nabla S)_y$ between the depths of 50 and 200 m is $(\nabla\theta \times \nabla S)_y = (13 \pm 2) \times 10^{-8}$ °C psu m^{-2} for transect D and $(\nabla\theta \times \nabla S)_y = (3.1 \pm 0.8) \times 10^{-8}$ °C psu m^{-2} for transect E, with $N^2 = (1.8 \pm 0.1) \times 10^{-5}$ s^{-2} for transect D and $N^2 = (2.5 \pm 0.1) \times 10^{-5}$ s^{-2} for transect E. The main uncertainty comes from the denominator of (36). From the arithmetic mean of depth averages H for stations 87, 88 and for 89, 90 we obtained H_D =

-9.6×10^{-7} °C psu m^{-2} and $H_E = -7.8 \times 10^{-7}$ °C psu m^{-2} for transect D and E, respectively. Collecting all the numerical values we obtained $v_D = 1.7$ cm s^{-1} for transect D, with the uncertainty interval (0.9/3.4) cm s^{-1} mainly resulting from H values dispersion for individual stations, and $v_E = 0.7$ cm s^{-1} for transect E, with the uncertainty interval (0.4/2.7) cm s^{-1}.

From Table 2 we estimated in the center of each transect at a depth of about 90 m:

$$\begin{aligned} \partial^2\theta/\partial z^2 &= 1.1 \times 10^{-4}\,^\circ\text{C m}^{-2}, \\ \partial^2 S/\partial z^2 &= -3.0 \times 10^{-5}\ \text{psu m}^{-2} \quad \text{for transect D} \\ \partial^2\theta/\partial z^2 &= 1.2 \times 10^{-4}\,^\circ\text{C m}^{-2}, \\ \partial^2 S/\partial z^2 &= -3.9 \times 10^{-5}\ \text{psu m}^{-2} \quad \text{for transect E.} \end{aligned}$$

Finally, using given above $(\nabla\theta \times \nabla S)_y$ values, the local velocity estimates are $v_D = (1.6 \pm 0.8)$ cm s^{-1} and $v_E = (0.3 \pm 0.2)$ cm s^{-1} applying the method relative to Eq. (26) and $v_D = (6.6 \pm 4.0)$ cm s^{-1} $v_E = (1.5 \pm 1.0)$ cm s^{-1} from Eq. (28). The main source of errors is uncertainty regarding the exact streamtube location, and the tracer spatial gradients. Further, all these concerns can be repeated for (26) and (28), which actually have rather large errors. This difficulty may, to some extent, be overcome by averaging the field variables over transects, as in (33). However, this procedure at least partially softens the gradient values, a fundamental difficulty also common to other hydrological estimates (Fig. 6).

Applying the algebraic viewpoint (9), formula (33) may be said to be a mere consequence of (26) and (28), and therefore the observed scattering of v estimates from (26), (28), and (33) needs some discussion. One explanation involves the smallness of $\partial^2\theta/\partial z^2$, the $\theta(z)$ profile being nearly linear, and this ultimately gives a large value $v_D \approx 6.6$ cm s^{-1}. In this context, a definite practical advantage is guaranteed by using (33) because of the nonsmallness of its denominator over a rather broad range of circumstances: indeed it becomes small only in a few cases, when both $\theta(z)$ and $S(z)$ are nearly linear at the same time.

We also applied Needler's formula (21) by fitting the potential density from Table 2 with

$$\rho = \frac{A}{6}z^3 + \frac{K}{2}z^2 + Byz + Cz + Dy + F.$$

This procedure gives the average northward velocity component: $v_D = 1.1 \pm 0.5$ cm s^{-1} for transect D and $v_E = 0.8 \pm 0.7$ cm s^{-1} for transect E. In this case also these estimates appear to be very sensitive, especially for transect E, to uncertainties over ρ data.

Finally, to validate our computations, we took θ–S data for transect D and calculated the velocity difference, ~ 4 cm s^{-1}, between the bottom and our more superficial depths using the thermal wind equation. Due to the complex structure of the density field with steep spatial gradients, this is probably underestimated. So, considering the value of 8 cm s^{-1} from Budillon et al. (2002) in station 88 near the bottom, at a depth of ~ 500 m, the northward velocity at our more superficial depths is ~ 4 cm s^{-1}, or even less, which matches the majority of our estimates, with the sole exception of that based on (28), the one discussed above.

8. Discussion

In this work Ertel's classical vorticity theorem is used for a class of potential vorticities relative to various materially conserved scalar quantities, also in the realistic case that a mild friction has to be considered. In the central part of our work chemically inert tracers and their potential vorticities are examined: we assume that the tracer time evolution is known, as is often the case in practice, and then try to identify the resulting velocity field.

Specifically, we investigate the question of the absolute velocity determination in a steady case relative to a streamtube, using the alongstream rate of change of some particular potential vorticity field. Our method can be seen as a generalization of Needler's (1985) classical arguments. A flow of well determined density field is then critically analyzed: in particular we infer the velocity field for nonhorizontal motions and recover Needler's formula related to a potential vorticity $\Pi_{fN^2} \approx -g\Pi_\rho$ for inclined flows. Indeed, the time rate of change of this Π_{fN^2} quantity is proportional to the vertical velocity component of the flow. Therefore, we show that $D\Pi_{fN^2}/Dt = 0$ for horizontal flows in hydrostatic approximation. Further, we show how this property holds also for any tracer potential vorticity Π_χ, associated with a materially conserved quantity χ.

For steady currents, if the potential temperature θ and salinity S can be considered as tracers, we also obtain an absolute velocity determination that essentially involves only first and second-order space derivatives of θ and S. This formulation allows one to account for friction and other forces acting on a fluid.

In the final part of the paper (section 6) it has been assumed that heat and salt are conserved in the sea, while momentum (vorticity) may be not conserved. It is well known that, unlike direct velocity observations, coarse-grained potential temperature and salinity fields are less contaminated by smaller-scale energetic eddies and internal waves. In strongly stratified marine layers the vertical momentum transport is much more efficient than that of heat and salt, the corresponding virtual (turbulent) Prandtl and Schmidt numbers typically being of the order of 10 (Jacobsen 1930; Taylor 1931; see also Turner 1973). We thus analyze the potential vorticities ratio $\Pi_\theta/\Pi_S \sim (\partial\theta/\partial z)/(\partial S/\partial z)$ for cases in which ρ is not easily determined. Again we find that

$$\frac{D}{Dt}\left(\frac{\Pi_\theta}{\Pi_S}\right) = 0$$

for horizontal flows. We thus obtain a formulation of steady water absolute velocity, which is later applied to a rather superficial current in the Ross Sea. This formulation seems appropriate in marine currents that are stratified both in salinity and temperature, with pronounced baroclinic turning of horizontal velocity with depth. In certain circumstances our approach may serve as a useful supplementary procedure to the existing methods of steady current absolute velocity determination, including the well-known beta-spiral method first proposed by Stommel and Schott (1977) and applied, for example, by Olbers et al. (1985) to the North Atlantic.

One further observation may be of some importance: for three main examples discussed, namely $\{\rho, \Pi_\rho\Pi_{fN^2}\}$, $\{\rho, \chi, \Pi_\chi\}$, and $\{\theta, S, \Pi_\theta/\Pi_S\}$, for steady horizontal motions (in hydrostatic approximation) the property of $D\Pi/Dt = 0$ is obtained, which implies these three types of potential vorticities are constant for this sort of motion. This statement appears to be complementary to our other results, which hold for essentially inclined fluid motions.

In synthesis we applied our formulas to various cases, both analytically and computationally, and actually discovered the profound difficulties associated with the method. Indeed, the streamtubes are usually difficult to identify, the flows are not steady, the data are of good quality only near the station, and so on. Therefore, finally we have to discuss the applicability of our ideas to realistic cases. There are several demands that experimental data have to fulfill in order to apply our method of absolute velocity determination successfully. These include quasi-steadiness and strong baroclinicity of the flow, its pronounced inclination to the horizon evident in the measured hydrological characteristics, as well as the existence of a comparatively dense observational network, with sufficiently small horizontal spacing between the stations for which CTD casts are available. Within these limitations, the method enables one to obtain a spectrum of the absolute velocity estimates, sometimes affected by substantial experimental errors, which should in any case be checked using direct current meter measurements. Similar considerations can also be applied to other estimates obtained, namely of the ratio of vertical and horizontal velocities, and in the search for the hydrologic no-motion level.

Acknowledgments

We must thank Agenzia Spaziale Italiana and SINAPSI for financial support and INFN for funding M.K's travel to Rome. We also thank Rossana De Gregorio, Laura Santonastaso, and Roberta Soldatelli for their enthusiastic collaboration.

REFERENCES

Baringer M. O., and J. F. Price, 1997a: Mixing and spreading of the Mediterranean outflow. *J. Phys. Oceanogr.*, **27**, 1654–1677. Find this article online

Baringer M. O., and J. F. Price, 1997b: Momentum and energy balance of the Mediterranean outflow. *J. Phys. Oceanogr.*, **27**, 1678–1992. Find this article online

Budillon G., S. Gremes Cordero, and E. Salusti, 2002: On the dense water spreading off the Ross Sea shelf. *J. Mar. Syst.*, **35**, 207–227. Find this article online

Cushman-Roisin B., 1994: *Introduction to Geophysical Fluid Dynamics*. Prentice Hall, 320 pp.

England M. H., and E. Maier-Reimer, 2001: Using chemical tracers to assess ocean models. *Rev. Geophys.*, **39**, 29–70. Find this article online

Ertel H., 1942: Ein neuer hydrodynamischer Wirbelsatz. *Meteor. Z.*, **59**, 277–281. Find this article online

Ertel H., and H. Kuehler, 1949: Ein Theorem ueber die stationaere Wirbelbewegung kompressibler Fluessigkeiten. *Z. Angew. Math. Mech.*, **29**, 109–113. Find this article online

Gill A. E., 1982: *Atmosphere–Ocean Dynamics*. Academic Press, 662 pp.

Godske C. L., T. Bergeron, J. Bjerknes, and R. C. Bundgaard, 1957: *Dynamic Meteorology and Weather Forecasting*. Amer. Meteor. Soc. and Carnegie Inst. Washington, 800 pp.

Haynes P. H., and M. E. McIntyre, 1987: On the evolution of vorticity and potential vorticity in the presence of diabatic heating and frictional or other forces. *J. Atmos. Sci.*, **44**, 828–840. Find this article online

Haynes P. H., and M. E. McIntyre, 1990: On the conservation and Impermeability theorems for potential vorticity. *J. Atmos. Sci.*, **47**, 2021–2031. Find this article online

Hide R., 1989: Superhelicity, helicity and potential vorticity. *Geophys. Astrophys. Fluid Dyn.*, **48**, 69–79. Find this article online

Hide R., 1996: Potential magnetic field and potential vorticity in magnetohydrodynamics. *Geophys. J. Int.*, **125**, 1–F3, *F*. Find this article online

Jacobsen J. P., 1930: The mixing of water masses in the sea. *Rapp. P.-V. Reun. Comm. Int. Explor. Sci. Mer Mediterr.*, **LXVII.**.

Kurgansky M. V., and I. A. Pisnichenko, 2000: Modified Ertel's potential vorticity as a climate variable. *J. Atmos. Sci.*, **57**, 822–835. Find this article online

Luyten J. R., J. Pedlosky, and H. Stommel, 1983: The ventilated thermocline. *J. Phys. Oceanogr.*, **13**, 292–309. Find this article online

Marshall J., D. Olbers, H. Ross, and D. Wolf-Gladrow, 1993: Potential vorticity constraints on the dynamics and hydrography of the Southern Ocean. *J. Phys. Oceanogr.*, **23**, 465–487. Find this article online

Müller P., 1995: Ertel potential vorticity theorem in physical oceanography. *Rev. Geophys*, **33**, 67–97. Find this article online

Needler G. T., 1985: The absolute velocity as a function of conserved measurable quantities. *Progress in Oceanography*, Vol. 14, Pergamon, 421–429.

Olbers D. J., M. Wenzel, and J. Willebrand, 1985: The inference of North Atlantic circulation patterns from climatological hydrographic data. *Rev. Geophys.*, **23**, 313–356. Find this article online

Pedlosky J., 1987: *Geophysical Fluid Dynamics*. Springer-Verlag, 710 pp.

Rhines P. B., 1986: Vorticity dynamics of the oceanic general circulation. *Rev. Fluid Mech.*, **18**, 433–497. Find this article online

Ripa P., 1981: Symmetries and conservation laws for internal gravity waves. *AIP Conf. Proc.*, **76**, 281–306. Find this article online

Roether W., V. Beitzel, J. Sueltenfuss, and A. Putzka, 1999: The Eastern Mediterranean tritium distribution in 1987. *J. Mar. Syst.*, **20**, 49–61. Find this article online

Salmon R., 1982: Hamilton's principle and Ertel's theorem. *AIP Conf. Proc.*, **88**, 127–135. Find this article online

Salmon R., 1998: *Lectures on Geophysical Fluid Dynamics*. Oxford University Press, 378 pp.

Salusti E., and R. Serravall, 1999: On the Ertel and Impermeability theorem for slightly viscous currents with oceanographic applications. *Geophys. Astrophys. Fluid Dyn.*, **90**, 247–264. Find this article online

Stommel H., and F. Schott, 1977: The beta spiral and the determination of the absolute velocity field from hydrographic station data. *Deep-Sea Res.*, **24**, 325–329. Find this article online

Taylor G. I., 1931: Internal waves and turbulence in a fluid of variable density. *Rapp. P.-V. Reun. Comm. Int. Explor. Sci. Mer Mediterr.*, **LXXVI,** 35–42. [Reprinted, 1960, *The Scientific Papers of Sir Geoffrey Ingram Taylor*, Vol. II, Cambridge University Press, 240–252.].

Turner J. S., 1973: *Buoyancy Effects in Fluids*. Cambridge University Press, 368 pp.

Wunsch C., 1978: The North Atlantic general circulation west of 50° West determined by inverse methods. *Rev. Geophys. Space Phys*, **16**, 583–620. Find this article online

Wunsch C., 1996: *The Ocean Circulation Inverse Problem*. Cambridge University Press, 442 pp.

APPENDIX A

9. A Special Case of Needler's Formula

Below we discuss a special case of Needler's formula (21) in which it allows an exact absolute velocity reconstruction through its own approximation. Calling $\Sigma = \log\rho$, formula (21) reads as

$$\mathbf{u} = \frac{g\mathbf{k}\cdot\nabla\Sigma\times\nabla\left(f\dfrac{\partial\Sigma}{\partial z}\right)}{\nabla\left(f^2\dfrac{\partial^2\Sigma}{\partial z^2}\right)\cdot\nabla\Sigma\times\nabla\left(f\dfrac{\partial\Sigma}{\partial z}\right)}\cdot\left[\nabla\Sigma\times\nabla\left(f\frac{\partial\Sigma}{\partial z}\right)\right]. \tag{A1}$$

As an example we take $f = f_0$ and

$$\Sigma = Az + C_1(\varepsilon x, y)\cos qz + C_2(\varepsilon x, y)\sin qz, \tag{A2}$$

where C_1 and C_2 are arbitrary functions, A is constant. The alongstream coordinate x is labelled by the parameter ε, and $q = \pi/d$, where d is the characteristic depth scale. From (A2) it follows that $\partial^2\Sigma/\partial z^2 = Azq^2 - q^2\Sigma$, and hence

$$\nabla\left(f_0^2\frac{\partial^2\Sigma}{\partial z^2}\right)\cdot\nabla\Sigma\times\nabla\left(f_0\frac{\partial\Sigma}{\partial z}\right) = f_0^2Aq^2\mathbf{k}\cdot\nabla\Sigma\times\nabla\left(f_0\frac{\partial\Sigma}{\partial z}\right)$$

since $\mathbf{k} \equiv \nabla z$. Dividing both numerator and denominator of (A1) by $\mathbf{k}\cdot\nabla\Sigma\times\nabla(\partial\Sigma/\partial z) \neq 0$ one has

$$\mathbf{u} = \frac{g}{f_0Aq^2}\left[\nabla\Sigma\times\nabla\left(\frac{\partial\Sigma}{\partial z}\right)\right], \tag{A3}$$

which is a divergence-free velocity that satisfies the basic equations (5) for $\alpha = \Sigma$ and $\beta = f_0\,\partial\Sigma/\partial z$ under approximation of incompressible fluid.

To be more specific, in (A2) we set $C_2 = 0$ and $C_1(\varepsilon x, y) = ayc(\varepsilon x)$. Here $c(\varepsilon x)$ describes possible weak dependence of Σ on x in the case of $\varepsilon \ll 1$ and the parameter a specifies the cross-stream density gradient. This flow mimics a marine front within the channel $-D \leq y \leq D$, with half-width D satisfying $aD \ll 1$, the latter reflects the smallness of the cross-front density gradients. For the hydrostatic stability of the flow it should be $\partial\Sigma/\partial z = A - cayq\sin qz < 0$ at any point or in any case $caD < |A|q^{-1} \equiv |A|d\pi^{-1}$.

The velocity x component, based on (A3), is

$$u = \frac{gca}{qf_0}\sin qz - \frac{gc^2k^2a^2}{f_0A}y. \tag{A4}$$

The first right-hand term in (A4) is merely the thermal wind, as follows from (A3) and the thermal wind relation $f_0(\partial u/\partial z) = -g(\partial\Sigma/\partial y)$. The second term interestingly shows the barotropic velocity contribution, which is predicted by Needler's formula (21), an example of a flow with uniform horizontal velocity shear

$$\frac{\partial u}{\partial y} = \frac{gc^2a^2}{f_0A}. \tag{A5}$$

For a numerical estimate we adopt $d = 1000$ m, $a^{-1} = 300$ km, $D = 30$ km, $c = 1$, $g = 9.81$ m s^{-2}, $f_0 = 1.41 \times 10^{-4}$ s^{-1}, and set $N^2 = -g(\partial\Sigma/\partial z) = -gA$ equal to 10^{-5} s^{-2}, which specifies the constant A. For these parameter values, the above hydrostatic stability criterion is always satisfied, the amplitude of the thermal wind component in (A4) becomes 7.4 cm s^{-1}, and the horizontal velocity shear (A5) is equal to 7.6×10^{-7} s^{-1}, which at $z = \pm D$ gives the barotropic velocity 2.3 cm s^{-1}, that is about 30% of the maximum baroclinic velocity contribution.

It can be shown that the solution (A2), (A3) satisfies the Bernoulli theorem for a steady flow, taken in the geostrophic approximation of “planetary scale” motions (Pedlosky 1987, section 6.20) consistent with formula (21). This analytical solution may be of interest as a particular model of outcropping isopycnal surfaces in the thermocline ventilation theory (cf.

Luyten et al. 1983).

APPENDIX B

10. Field Data off Gibraltar

The Baringer and Price field data (1997a,b), relative to their transects A, C, and F (Fig. B1) downstream from the strait of Gibraltar, are now discussed in more detail. In Table 1 we estimate the main physical quantities of this outflow, denoting as "central region" the one characterized by the highest velocities, and with $S > 36.4$ psu, as computed by Baringer and Price (1997a,b). We use (26)–(27) since S is better defined than θ, and this implies smaller uncertainties.

We also computed the local estimate of $\mathbf{u}$, as expressed in the last member of equations (26) and (28). These estimates have the considerable advantage that they can be computed using more "local" hydrologic data, but in so doing it is difficult to avoid large errors. Similar considerations can be repeated for $\mathbf{F}/\rho$, which we estimate as $(\boldsymbol{\tau}_B + \boldsymbol{\tau}_I)/h\rho$ using the Baringer and Price (1997) notations, $\boldsymbol{\tau}_B$ and $\boldsymbol{\tau}_I$ being viscous stresses on the sea bottom and current interface, respectively. The *curl* of the frictional force is approximated here by

$$\boldsymbol{\nabla} \times \frac{\mathbf{F}'}{\rho} \approx \frac{1}{h}\mathbf{k} \times \frac{\mathbf{F}}{\rho}$$

and is directed in a nearly horizontal cross-stream direction. All this ultimately means that the inviscid part of the velocity is (0.5–0.2) m s^{-1} and the viscous component is −(0.05–0.10) m s^{-1} with errors of 20%–100%, largely due to angle uncertainties (see Table 1); all this is in agreement with the experimental dataset.

In addition, the steady velocity component due to salt and temperature diffusive effects, characterized by the vertical turbulent diffusivity coefficient κ, can interestingly be determined from (12) by $|\mathbf{u}^*| = \kappa H/(\nabla\theta \times \nabla S)_y$; see other notations in section 7. From (36) it now follows that the ratio of this additional and main alongstream component is merely $|\mathbf{u}^*|/|\mathbf{u}| = \kappa N^2/f\mathbf{u}^2$, which is less than 1% if $\kappa \sim 10$ cm^2 s^{-1}.

In synthesis we see that the best estimates can be obtained using the most precisely defined set of data and "nonlocal" equations. On the other hand, if Π_θ and Π_S do not vary significantly between two transects, large experimental errors can prevent (26) and (28) being used in practice. Note however that our knowledge of the experimental dataset is only partial and all these estimates must be considered only a demonstration of general applicability of our relations. A more accurate estimate requires a detailed knowledge of the original dataset, as shown in section 7 for currents in the Ross Sea.

Tables

TABLE 1. Values relative to the bottom current flowing off Gibraltar, estimated from the Baringer and Price (1997a,b) dataset. In this table the first part comes from direct estimates taken from Baringer and Price (1997a,b), often without errors, although uncertainties of ~ 10% may reasonably be assumed. The values of $\nabla\theta$ and ∇S are the values of θ and S in the center of the current, minus the value along the $S = 36.4$ psu surface, over h. In the same way we have tentatively estimated the angles between $\nabla\theta$ and ∇S. Finally, c_D is usually taken to be 5×10^{-3} (MKS units), but the total stress (bottom and interfacial) from Baringer and Price (1997a,b) is about twice their bottom stress (in their Fig. 6a), given $c_D = (2–12) \times 10^{-3}$ (MKS units); so we assumed $c_D = 0.02$ (MKS units) (rht = right-hand term)

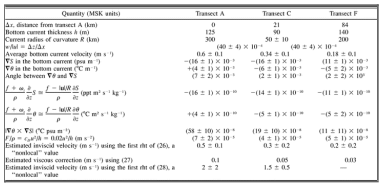

Click on thumbnail for full-sized image.

TABLE 2. Synthesis of hydrologic data obtained during the X Italian Expedition in the Ross Sea (CLIMA Project); see Budillon et al. (2002) for more details

200	1.2	34.71	27.77
	(b) Station 88		
25	−1.15	34.03	27.36
50	−1.3	34.20	27.52
75	−1.3	34.27	27.57
100	−1.28	34.31	27.61
150	−0.95	34.46	27.70
200	−0.8	34.53	27.75
	(c) Station 89		
25	−1.5	33.67	27.07
50	−1.5	33.96	27.33
75	−1.4	34.20	27.51
100	−1.2	34.27	27.58
150	−0.5	34.40	27.64
200	0.7	34.58	27.73
	(d) Station 90		
25	−1.25	34.02	27.35
50	−1.28	34.02	27.36
75	−1.2	34.07	27.39
100	−1.0	34.20	27.49
150	−0.6	34.42	27.63
200	−0.4	34.49	27.67

Click on thumbnail for full-sized image.

Figures

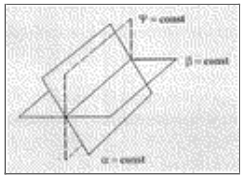

Click on thumbnail for full-sized image.

FIG. 1. Sketch of steady streamlines viewed as the intersection of α, β, Ψ, … planes

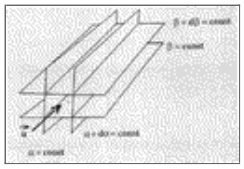

Click on thumbnail for full-sized image.

FIG. 2. An (α, β) tube

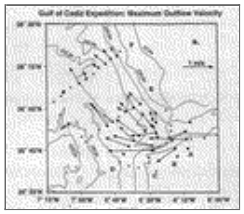

Click on thumbnail for full-sized image.

FIG. 3. General geographical situation and position of transects A, C, and F observed by Baringer and Price (1997a,b) off Gibraltar. Depths are in fathoms

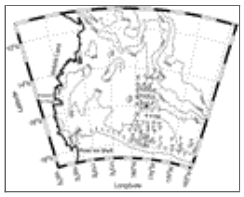

Click on thumbnail for full-sized image.

FIG. 4. Mooring (triangle) and CTD cast (dots) positions in the Ross Sea (Antarctica); depths are in meters, depths below 500 m are shaded. The density vertical fields of the transects D–E are discussed in the text and shown in Fig. 5. More details on the hydrological field are in Budillon et al. (2002)

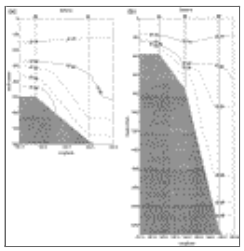

Click on thumbnail for full-sized image.

FIG. 5. Vertical sections of potential density (kg m^{-3}) relative to (a) transects D and (b) transect F observed in the Ross Sea (Antarctica). More details are in Budillon et al. (2002)

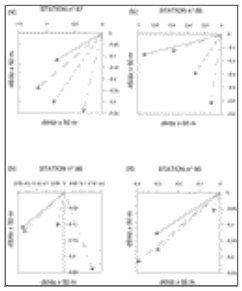

Click on thumbnail for full-sized image.

FIG. 6. Hodograph of pseudovector $\mathbf{U} = (\partial\theta/\partial z \times 50\ \text{m}, \partial S/\partial z \times 50\ \text{m})$ for stations (a) 87, (b) 88, (c) 89, and (d) 90. Solid arrow corresponds to a depth of 150 m, dashed arrow to 115 m, small dashed arrow to 75 m, and dashed–small-dashed arrow to 50 m

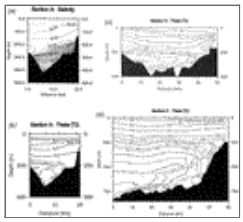

Click on thumbnail for full-sized image.

FIG. B1. Hydrologic properties relative to transect A [(a) salinity, (b) temperature] and relative to transects (c) C, and (d) F (temperature) observed by Baringer and Price (1997a,b) off Gibraltar

* On leave from A. M. Obukhov Institute of Atmospheric Physics, Russian Academy of Sciences, Moscow, Russia

Corresponding author address: Dr. Ettore Salusti, INFN-Dip. di Fisicà, Universita La Sapienza, Piazzale A. Moro 2, Roma 00185, Italy. E-mail: ettore.salusti@roma1.infn.it

top